Electronic Supplementary Material (ESI) for Physical Chemistry Chemical Physics.

Do Primary Carriers of Both Positive Charge and Unpaired Electron Spin exist in Irradiated Propylene Carbonate?

V.I. Borovkov,[1,2,*]

[1] *Voevodsky Institute of Chemical Kinetics and Combustion, Siberian Branch of Russian Academy of Science, 3, Institutskaya st., Novosibirsk 630090, Russia*

[2] *Novosibirsk State University, 2 Pirogova st., Novosibirsk 630090, Russia*

* *Corresponding author: fax: 7-(383)330-73-50; E-mail: borovkov@kinetics.nsc.ru*

Electronic Supporting Information

1. Dependence of the geminate recombination probability on a medium polarity

The probability of geminate recombination in irradiated propylene carbonate (PC) exhibiting $\varepsilon(293\ K)\approx65$seems to be vanishingly small. Indeed, the average distance, R, between the primary charge carriers in organic media is about of several nanometers [S1, S2]. In liquids, the probability of the recombination of an isolated RIP is usually estimated as $exp(-R/R_O)$, where $R_O=e^2/\varepsilon kT$ is the Onsager radius [S1, S2]. The latter equals approximately to 56(nm)/ε at room temperature and does not exceed the typical R values at the dielectric constant $\varepsilon>20$. It is also known that the free ion yield in PC is close to saturation plateau that is observed at further increase in dielectric constant [S3]. This fact might be interpreted as that almost all created ion pairs escape the geminate recombination in media with such high dielectric constants.

However, the abovementioned Onsager's result has been obtained for sizeless charges. In the extreme polarity limit, when the long-range interaction of ions can be neglected, two particles, which were initially separated by the distance R, would encounter at the contact radius of $a<R$ with a probability as large as a/R [S4]. This probability is not a negligible value if the distance of the irreversible recombination of RIPs amounts to about of 1-1.5 nm.

The only way to estimate accurately the geminate recombination probability in the conditions of a radiation experiment is a computer modelling of diffusion and drift motion of ions in a radiation spur. Such modelling has been performed using the model of radiation-induced processes suggested in ref S5. In the cited work, it was shown that an average spur formed upon 20 keV X-ray irradiation in liquid dodecane was of a 5-9 nm radius and contains initially 4-5 ion pairs. The starting distribution of distances between the ions in each pair was described by an exponent with a mean distance between the particles as large as 4.5 nm. Ion recombination radius was assumed to be equal 1 nm. The role of the solvent polarity was estimated performing all the calculations for two variants differing only by the value of dielectric constant, 2 or 65, of the continual medium.

During the modelling, geminate recombination events involving ions initially created as the same ion pair, $F_G(t)$, were recorded separately from other, cross recombination events, $F_C(t)$. An involvement of excited states as well as of neutral radicals was neglected. Here, we present results obtained for the ion's mobility equalled to 10^{-4} cm^2/Vs that are expected for molecular ions in a solvent with the viscosity of 2-3 cP. Trial calculations showed that the usage of more complicated models with changing carriers mobility or the formation of secondary ions due to scavenging the primary ones does not affect the proportion between $F_G(t)$ and $F_C(t)$ dependences except for very early times. The use of the distribution function of other shapes with the similar mean distance between primary ions would give rise to some variations in the calculation results, but these changes are non-essential for the present work.

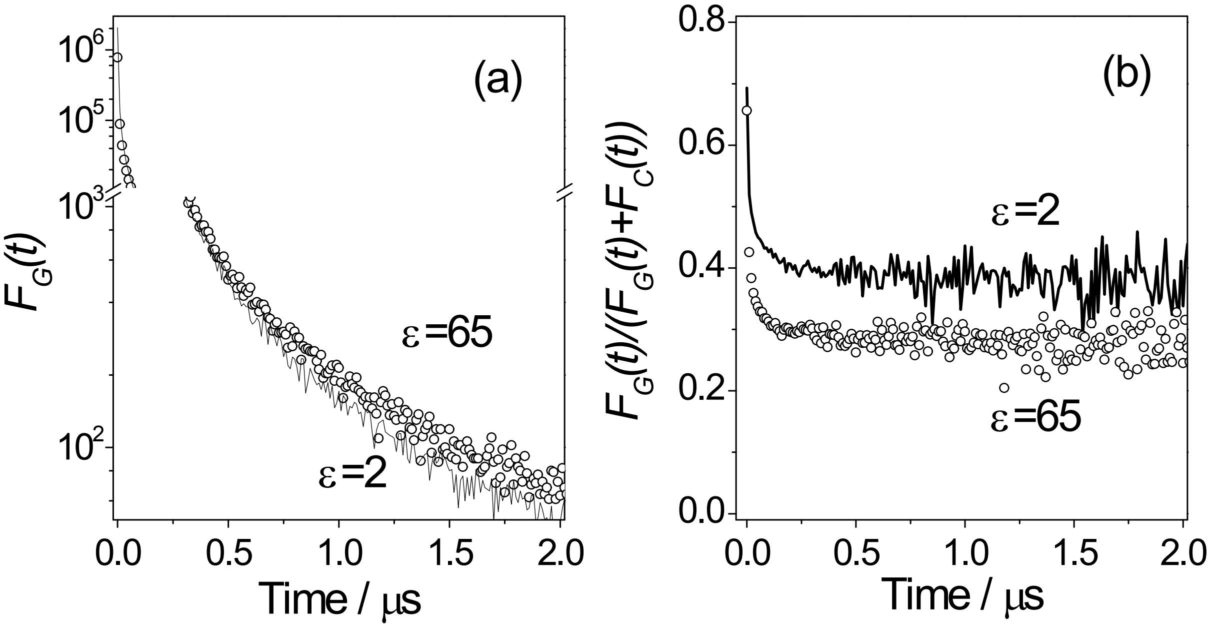

Fig. S1. a) Calculated recombination rate, $F_G(t)$, of geminate ion pairs for the spur described in the text in the case of low (line) and high (circles) polarity of medium; b) Fraction of geminate ion pairs, $F_G(t)$, among all recombining pairs $F_G(t)+F_C(t)$ at the solvent polarity indicated in the graph.

Fig. S1a shows on the semilogarithmic scale the calculated rates of the geminate recombination, $F_G(t)$, for both the cases. Note that at the higher polarity, the recombination rate of *geminate* pairs becomes, after a time, *higher* as compared to the medium with a lower polarity. This result does not contradict to the much larger, *ca*. 44%, calculated free ions yield at ε=65 as compared to *ca*. 2.5% at ε=2, since, though it is hard to see from the figure, more than half of the ion pairs in the non-polar solvent recombine within the first 10 ns. Partially, this effect originates from the exponential shape of the distribution function of initial distances between primary charge carriers.

Fig. S1b shows that the plateau levels of the fraction of the geminate RIPs among all recombining pairs at more or less realistic conditions are comparable for both low and high medium polarity. In any case, the geminate recombination probability is not reduced as dramatically as could be expected on the basis of the familiar Onsager's formula after the great increase in the solvent polarity.

References to the section 1

S1. Mozumder, A. *Fundamentals of Radiation Chemistry*. Academic Press, San Diego CA, USA, 1999.

S2. Schmidt, W. F. *Liquid State Electronics of Insulating Liquids*. Boca Raton, Florida: CRC Press, Inc. 1997.

S3. Jay-Gerin, J.-P.; Ferradini, C. On The Variation Of The Free-Ion Yield With The Static Dielectric Constant In The Radiolysis Of Liquids. *Radiat. Phys. Chem*. **1989**, 33, 251-253.

S4. Tunitskii, N. N.; Kaminskii, V. A.; Timashev, S. F. *Methods of Physicochemical Kinetics*. Khimiya, Moscow, 1972 (in Russian).

S5. V. I. Borovkov, K. A. Velizhanin. Experimental and Computer Simulation Study of Delayed Fluorescence Decay from Irradiated n-Dodecane Solutions of TMPD. *Radiat. Phys. Chem*. **2007**, 76, 998–1010.

2. **Backgrounds of the method of time-resolved magnetic field effects**

The correlation between spins of electrons, which fill a closed electronic shell in a molecule, is kept after separating these electrons upon ionization of the molecule. The remaining correlation is the base of the phenomenon of the magnetic field effects in the recombination fluorescence of radical ion pairs (RIPs). In zero magnetic field (see Scheme S1), the spin states of a RIP are nearly degenerate thus facilitating equilibration of the populations of all these states due to hyperfine couplings (*HFCs*) as well as to phase paramagnetic relaxation [S6, S7].

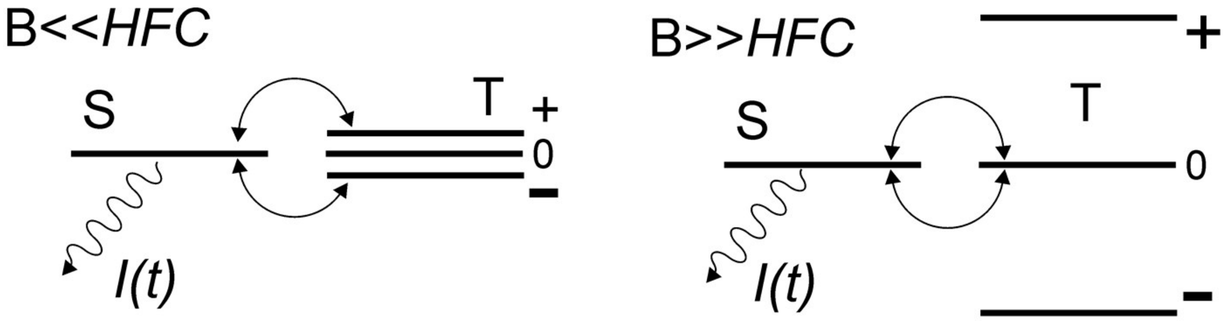

Scheme S1. Singlet (S) and triplets (T_+,T_0,T_-) spin sub-levels of a radical ion pair in a small (left part) and in a strong magnetic field (right part) neglecting spin-spin interactions between the partners. Arrows show S-T mixing due to hyperfine couplings as well as phase paramagnetic relaxation in the radical ions. The wavy line is to emphasize that fluorescence can appear only due to the recombination of the RIP in its singlet state.

In a relatively strong magnetic field, these interactions as well as Zeeman interactions of the radicals composing the RIP, result in mixing of the singlet with, roughly speaking, single triplet state, T_0, only. Therefore, if the singlet spin state population were monitored via fluorescence from the S-state then, in the idealised situation with neglecting spin-lattice relaxation, the intensity of the recombination fluorescence after singlet-triplet mixing would increase by up to a factor of 2 as a response to turning the magnetic field on.

The above picture is valid only for an isolated RIP, while in the radiation track some RIPs recombine being composed of radical ions created due to ionization of different molecules. In such RIPs, no essential initial spin correlation could be expected. As the first approximation, the pulsed irradiation of a luminophore solution results in the decay of the recombination fluorescence intensity, $I(t)$, which is proportional to the recombination rate of the RIPs in the singlet spin state:

$$I(t) \propto F_G(t) \cdot \rho_{SS}(t) + F_C(t)/4 \approx [\theta \cdot \rho_{SS}(t) + (1-\theta)/4] \cdot [F_G(t) + F_C(t)] \qquad (S1)$$

Here $F_G(t)$ and $F_C(t)$ are the recombination rates of RIPs of different types as determined above that are believed to be independent on an external magnetic field. $\rho_{ss}(t)$ is the time dependence of the singlet state population of the initially singlet-correlated RIPs; the uncorrelated RIPs are in the singlet state with the probability of 0.25. In eq. (S1), the second approximate equality was derived assuming that the fraction $\theta = F_G(t)/[F_C(t)+F_G(t)]$ of the spin-correlated, “geminate” RIPs does not vary significantly with time. For some time ranges, this assumption can be substantiated with a computer modelling like presented above.

Because of complexities related to the experimental determining the RIPs’ recombination kinetics, it is much more convenient to study the ratio of recombination fluorescence decays, $I_B(t)$ and $I_0(t)$, recorded at the strong and zero magnetic fields, respectively. This ratio is referred to as the time-resolved magnetic field effect (TR MFE):

$$\frac{I_B(t)}{I_0(t)} \approx \frac{\theta \cdot \rho_{SS}^{B}(t) + (1-\theta)/4}{\theta \cdot \rho_{SS}^{0}(t) + (1-\theta)/4}, \tag{S2}$$

where superscripts B and 0 point to strong and zero external magnetic fields, respectively. The $\rho_{ss}(t)$ dependence can be calculated analytically for some particular cases as presented below.
Of course, the observability of TR MFE in experiments also depends on many other factors like the paramagnetic relaxation, strong spin-orbit or exchange interactions as well as the separation of electron spin and electric charge due to chemical processes.

The RIP’s singlet state population, $\rho_{ss}(t)$, can be evaluated at the magnetic field B as previously suggested (see, e.g. [S6, S7]):

$$\rho_{ss}^{B}(t) = \frac{1}{4} + \frac{1}{4} exp\left(-\frac{t}{T_1}\right) + \frac{1}{2} exp\left(-\frac{t}{T_2}\right) cos(\frac{\Delta g \beta B}{\hbar} \cdot t) \cdot G_c^B(t) G_a^B(t) \tag{S3}$$

,

$$\rho_{ss}^{0}(t) = \frac{1}{4} + \frac{3}{4} exp\left(-\frac{t}{T_0}\right) G_c^0(t) G_a^0(t) \tag{S4}$$

,

where $1/T_{1,2} = 1/T_{(a)1,2} + 1/T_{(c)1,2}$ are the sums of the longitudinal and phase relaxation rates of the RIP partners; T_0 is the parameter to describe phase relaxation in a zero magnetic field in the same manner; Δg denotes the difference between the g-values of the RIP partners; β is the Bohr magneton. Subscripts “*a*” and “*c*” are to indicate that a particular parameter relates to radical anion and radical cation, respectively.

In this work, the contribution of *HFC* to the spin dynamics was calculated using the semi-classical approximation [S8] of functions $G(t)$ as the following in the field units for σ,

$$G^0(t) = \frac{1}{3} \cdot [1 + 2 \cdot (1-(\gamma\sigma t)^2) \cdot \exp[-(\gamma\sigma t)^2/2)], \tag{S5}$$

$$G^B(t) = \exp[-(\gamma\sigma t)^2/2)], \tag{S6}$$

where σ^2 is the second momentum of the radical ion EPR spectrum, $\gamma = g\beta/\hbar$ is the electron gyromagnetic ratio.

To visualize the effect of σ and Δg, in Fig. 2S two calculated TR MFE curves are shown for the case of a RIP, which is composed of partners exhibiting unresolved EPR spectra with, conditionally, σ_c=0.3 mT and σ_a=0.1 mT. One of the curves was calculated at Δg=0 while another one was done at Δg=0.003 (B= 1T). At negligible Δg value, the peaks in the TR MFE curve are located at nearly $1/\gamma\sigma$ if σ_c and σ_a values are different [S7]. The obvious difference between the TR MFE curves is due to the cosine term in Eq. (S3), which provides an oscillatory behavior in strong magnetic fields. The oscillations decay on a time scale determined by the characteristic time of the singlet-triplet mixing caused by HFC, that is of the order of inverse EPR spectrum width in frequency units.

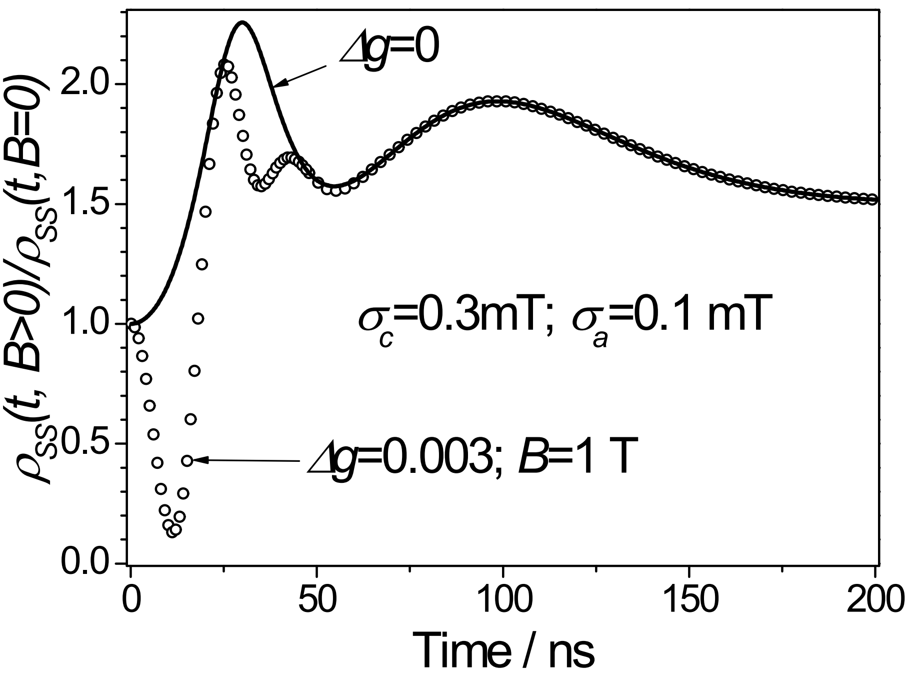

Fig. S2. Calculated TR MFE curves for singlet-born (θ=1) radical ion pairs ensemble in the absence of paramagnetic relaxation. Parameters are σ_c=0.3 mT and σ_a=0.1 mT; Δg=0 (line) or Δg=0.003 (circles) at B=1 T.

For the modeling of experimental data, the second moments of the spectrum, σ^2, for radical ions of perdeuterated *para*-terphenyl (*p*TP-d_{14}) were calculated using the data on the *p*TP-h_{14} [S9, S10]. The σ value amounted to 0.074 mT and 0.069 mT for the radical cation and the radical anion, respectively. Note that the g-values for the *p*TP radical ions are very close to each other and amount to *ca*. 2.0028.

References to the section 2

S6. Bagryansky, V.A.; Borovkov, V.I.; Molin, Y.N. Quantum beats in radical pairs. *Russ. Chem. Rev*. **2007**, 76, 493-506.

S7. Borovkov, V.; Stass, D.; Bagryansky, V.; Molin, Y. Study of Spin-Correlated Radical Ion Pairs in Irradiated Solutions by Optically Detected EPR and Related Techniques. In: *Applications of EPR in Radiation Research*, Ed. by Lund, A. and Shiotani, M. Eds.; Springer International Publishing: Cham, Switzerland, **2014**, 629–663.

S8. Schulten, K.; Wolynes, P. G. Semiclassical Description of Electron Spin Motion in Radicals Including the Effect of Electron Hopping. *J. Chem. Phys*. **1978**, 68, 3292-3297.

S9. Berndt, A.; Jones, M.T.; Lehnig, M.; Lunazzi, L.; Placucci, G.; Stegmann, H.B.; Ulmschneider, K.B. *Landolt-Börnstein. Numerical Data and Functional Relationships in Science and Technology. Organic Anion Radicals.* New Series, Subvolume 9d1. Springer-Verlag: Berlin, Heidelberg. 1980.

S10. Courtneidge, J.L.; Davies, A. G.; McGuchan, D. C. The Electron Spin Resonance Spectra of the Radical Cations of p-Terphenyl, Triphenylene and Triptycene. *Recl. Trav. Chim. Pays-Bas* **1988**, 107, 190-196.